

# **Six Years of Performance Monitoring of A Geogrid Reinforced Test Section on an Alberta Highway**

Jhuma Saha, M.Sc., P.Eng.,  
Pavement Design Engineer  
Alberta Transportation

Mohammad Karim, M.A.Sc., P.Eng.,  
Surfacing Standard Specialist  
Alberta Transportation

Marta Juhasz, B.A. Sc., P.Eng.,  
Director, Pavement Engineering  
Alberta Transportation

Paper Prepared for presentation at the “Testing and Modeling of Roadway/Embankment Materials and Geotechnical Engineering session”

2022 TAC Conference & Exhibition

## **ABSTRACT**

Many studies indicate that geosynthetic reinforcement can help prolong the service life of a flexible pavement by reducing the required structural number of the pavement, and improving rutting resistance and subgrade capacity. However, not enough long-term geosynthetic field performance studies are available to help understand the benefits of reinforcing a pavement on a reasonably good subgrade soil. To that end, in 2015, Alberta Transportation constructed a geogrid reinforced test section on Hwy 63 north of Wandering River. A contiguous segment of the highway with the same pavement structure, environment, traffic, and similar subgrade was selected as an unreinforced control section against which to compare field performance. This highway is the major route to Fort McMurray and the oil sands and carries annual average daily traffic (AADT) of 4,000, with approximately 28 percent trucks. The highway is part of the oversize overload highway network and sees some very unique truck and axle configurations. The pavement structure of the geogrid reinforced test and unreinforced control sections was designed for staged construction. The second (or final) stage pavement was delayed to accelerate pavement distress development and pavement performance comparison.

Performance data such as International Roughness Index (IRI), rutting measurements, Laser Crack Measurement System (LCMS), Falling Weight Deflectometer (FWD), and pavement surface condition from visual inspections were collected for six consecutive years. These data were analyzed for both the geogrid reinforced test section and the unreinforced control section. This study did not find any significant differences in the analyzed data or visual condition between the reinforced and the unreinforced sections over six years. This paper has also attempted to investigate the possible reasons behind these findings. Both sections have reached a condition where further delay in final stage pavement construction would be imprudent. The longer-term performance will be monitored after the final stage pavement construction and reported in the future to confirm the findings.

## **1. BACKGROUND**

Numerous studies document the benefits of geogrid stabilization in aggregate base layers. These reported benefits include improving the modulus or stiffness, and reducing the permanent deformation of pavement. However, some long-term performance studies of geogrid stabilized pavements are available in the literature.

A test section with geogrid and an adjacent control section without any reinforcement were constructed on highway 63 control section 06 (hwy 63:06) on the northbound lane (NBL) to evaluate the geogrid performance. A multi-axial hexagonal structure and triangular aperture geogrid (Tensar TX5) was installed on top of the compacted subgrade and below the granular base layer in the geogrid reinforced test section. The reinforced test section limits are from kilometer (km) 18.170 to km 18.870 and the unreinforced control section limits are from km 18.870 to km 19.590. The length of each section is 710 meters (m). Both the reinforced test and unreinforced control sections have a similar profile, cross-section, and construction history. The pavement construction was completed in June 2015. Both geogrid reinforced test and unreinforced control sections have a first-stage pavement of 130 mm Asphalt Concrete Pavement (ACP) on 400 mm Granular Base Course (GBC).

Hwy 63:06 NBL from km 0.160 to km 27.540 was based and first stage paved in 2015 and the final paved in 2017. However, final paving was delayed on the reinforced geogrid test and unreinforced control sections to evaluate the geogrid performance, although final paving was inadvertently placed on a short segment of the geogrid test section from km 18.170 to km 18.245.

This paper documents the performance of the geogrid test section that was assessed through International Roughness Index (IRI), rutting measurements, Laser Crack Measurement System (LCMS), Falling Weight Deflectometer (FWD) as well as field observations of the existing surface condition. The results are also compared with the adjacent unreinforced control section.

## 2. LITERATURE REVIEW

Many studies have been performed in the past few decades to investigate the effect of geosynthetics both geogrids and geotextiles reinforcement on pavement performance. These studies include a variety of laboratory experimental techniques comprising of repeated triaxial load tests; laboratory cyclic load tests; full-scale field studies encompassing field cyclic plate load tests and field accelerated load tests; finite element (FE) numerical model developments; etc. These studies report various findings and are summarized as follows.

A review of full-scale field studies carried out by Alimohammadi et al. [1] attempted to compare the findings of a number of field studies by different investigators. This review revealed that the main appreciable improvement of geosynthetic both geogrid and geotextile reinforcements depends on various aspects such as subgrade stiffness, base aggregate thickness and quality, ACP thickness and quality, geogrid stiffness and location, etc. Alimohammadi developed a formula to calculate the granular equivalent (GE) factor from FWD tests for unreinforced and geosynthetic reinforced sections of the experimental tests by various investigators. The GE factor could be used by the designers to evaluate the effects of geosynthetics on pavement performance.

Perkins S.W. [2] performed research on the geosynthetic reinforcement of flexible pavement using laboratory-based pavement sections. Two different biaxial geogrid and one geotextile were used in this study. This study found that identical size and composition but stiffer geosynthetic provides better pavement performance. Other findings from this study revealed that geosynthetic reinforcement of the test sections with 75 mm of asphalt, and 200 to 375 mm thickness of the base materials provided important benefits when the subgrade had a CBR of 1.5 or less, and little to no benefits were noted when the subgrade had a CBR of 20 or more. Although subgrade soil with CBR between 1.5 and 14 was not tested in this study. The study also indicates that the placement position of reinforcement is an important design consideration.

Some experimental studies were performed on both single-layer and multi-layer geogrid reinforced sections. For instance, Cancelli and Montanelli [3] found that multilayer geogrids show lower deformation than the common single-layer geogrid.

Ibrahim et al. [4] conducted laboratory testing on five pavement prototype sections and FE analysis to explore the effectiveness of geogrid reinforcement on the flexible pavement. These sections consisted of 50 mm ACP, 150 mm GBC, and a 300 mm clay subbase. Static plate load testing was performed and results were compared with the control section with no reinforcement. These results revealed that the optimum position of the geogrid to reduce tensile strains was found directly underneath the ACP layer and also within 33 to 50 % of the GBC layer height measured from the bottom of the GBC.

Haas et al. [5] performed a laboratory-based research program comprising to explore the effects of geogrid reinforcement of granular base layers of flexible pavement. The tests involved full scale cyclic load tests on model pavement sections including varying thickness of reinforced and unreinforced granular bases, variable reinforcement location, and subgrade strength. The findings of that research reveal that

for high-deformation systems both fabric and geogrid can be effective in tension membrane action, but for low-deformation systems, the interlock and confining action of a grid is required to provide effective reinforcement. The work showed that permanent deformation of both types of systems can be significantly reduced by using geogrid reinforcement in the granular base. This study concluded that, for optimum effect, geogrid reinforcement should be placed at the base-subgrade interface of thin base sections and near the middle of thicker bases. Moreover, the zone of geogrid placement should not involve elastic tensile strains in the geogrid that are greater than 0.2 %. The study concluded that under the ideal condition of geogrid placement, geogrid reinforcement can be highly effective in reinforcing the granular base material and thereby extend the life of the structure.

Chen et al. [6] quantified the structural contribution of geogrid reinforcement in terms of increasing the resilient modulus of the base course layer and reducing the thickness of the base aggregate layer in the pavement structure. The results from the cyclic plate load tests conducted in this study indicated that the value of the resilient modulus of the base course layer can be increased by 10-90 percent and that the thickness of the base layer can be reduced by 12 to 49 percent for the geogrid reinforced pavement sections.

Ghafoori et al. [7] performed an experimental laboratory program to assess the effectiveness of biaxial and triaxial geogrid reinforced flexible pavements to reduce the roadway section. Six laboratory tests were conducted with two different base thicknesses (305 mm and 406 mm) and the same asphalt thickness. Geogrid was placed at mid-depth of thicker aggregate base layer sections and at the subgrade-base interface of the thinner base layer sections. The instrumentations included pressure cells placed at different locations of the test sections, foil strain gauges installed on the ribs of geogrids, and Linear Variable Differential Transformer (LVDT) placed on top of the loading system. Test results revealed that the inclusion of both biaxial and triaxial geogrids in flexible pavement reduced the Asphalt surface rutting and vertical stresses at the subgrade-base interface. Using the results of rutting depth, it was found that the use of geogrid increased the number of load applications by a factor of 1.5 to 7 depending on the test section and geogrid type. Using a Base Course Reduction (BCR) method and the measured rutting depth, the inclusion of geogrid resulted in the base thickness reductions of 11 to 44 percent depending on the variables.

A study by Siekmeier, J. [8] concluded that geogrids provide benefits and that this benefit varies during the year. This study recommended that the seasonal effects be included during implementation. This would allow the fatigue and rutting to be more accurately estimated over the expected pavement design life. The conclusions were based on field and laboratory testing combined with numerical analyses performed using both PFC3D and MnPAVE software.

Moghaddas-Nejad et al. [9] conducted tests using a facility that allowed repeated passes of a tire across a section of pavement that was either unreinforced or reinforced with a geogrid. Surface deformations, internal movement in the pavement, and subgrade deformation were measured. The study indicated that confinement and interlocking of the base materials as well as the improved load distribution on the subgrade layers are the main causes of reduction of subgrade deformation. Both single and multiple track tests were performed. In both cases, for a thin base layer, the least surface deformation was obtained with the geogrid at the center of the base layer.

Zadehmohamad et al. [10] developed a FE model to evaluate the benefits of geosynthetic reinforcement on flexible pavements. This study indicated that the inclusion of one geogrid/geotextile layer at the base-subgrade interface could significantly reduce pavement rutting. Other findings include the use of geogrid

is more effective than geotextile in reducing pavement rutting, and superior benefits were noted in using double geogrid layers compared to single layer cases. The calculated Traffic Benefit Ratio (TRB) value from this study demonstrates an optimum at a base thickness of 250 mm.

A study by Webster, S.L. [11] indicated that geogrid performance is a function of the depth of geogrid placement. The use of geogrid can reduce the total pavement design thickness. The thickness reduction range from approximately 40 percent for unreinforced pavement thicknesses of 11 inches (279 mm) to 5 percent for 30 inch (762 mm) thick pavements.

A study by White, D. J., et al. [12] to assess the performance of geogrid stabilized base layer under asphalt pavement using cyclic plate load testing found that there is about 11 percent increase in the composite resilient modulus ( $M_{r-comp}$ ) of a geogrid section than in unreinforced control section. A similar analysis of the FWD test results did not show the statistically noteworthy benefit with the inclusion of geogrid. The ( $M_{r-comp}$ ) was measured on the ACP surface.

A tabular summary of the literature review, presenting details of pavement layers, geogrids tested and key finding, is presented in Appendix 1. While difficult to compare, based on the literature review, geogrids provide the most structural benefit when subgrades are weaker (CBR less than 8) and when the pavement layers are thinner (less than 100 mm ACP, less than 300 mm GBC), and that the location of the geogrid within the structure plays a key role and is better mid-GBC for thicker GBC layers (300 mm or greater).

### **3. GEOGRID INSTALLATION AND AUTOMATED PLATE LOAD TESTING DURING CONSTRUCTION**

The geogrid work component was completed in June 2015, and Automated Plate Load Testing (APLT) and Dynamic Cone Penetrometer (DCP) testing were conducted in the field to evaluate in situ performance of the reinforced test and unreinforced control section. Multiple APLT tests were performed on either the first 200 mm layer of GBC, or on the second 200 mm layer of GBC, using a 12 in. (305 mm) diameter plate. In total there were eleven test locations in the geogrid reinforced test section and four test locations in the unreinforced control section. DCP testing was also conducted at each APLT location. At one location in geogrid reinforced test section and unreinforced control section, APLT and DCP testing was performed directly on the subgrade. The majority of tests were conducted at the same locations on the top of first and second lifts of GBC. Tests were performed using 10,000 cycles at one location each in unreinforced control and geogrid reinforced test sections and 1,000 cycles at all remaining locations.

Results showed:

- Based on DCP testing, the top 300 mm of subgrade was stiff with an average subgrade California Bearing Ratio (CBR) of 37 in the geogrid section and 44 in the unreinforced control section (the CBR range was 20 to 55).
- Based on the one location of APTL testing of the subgrade each, the resilient modulus ( $M_r$ ) of the subgrade was 276 MPa in the geogrid test section and 627 MPa in the unreinforced control section.
- Based on DCP testing of the first 200 mm of GBC, the average CBR in the GBC layer ranged from 29 to 59 in the geogrid test section and 40 to 87 in the unreinforced control section.
- For the 1,000 cycle APTL testing, the in-situ average composite resilient modulus ( $M_r$ ) in the geogrid section was about 660 MPa and in the unreinforced control section was about 950 MPa.

- The ratio of base layer to subgrade  $M_r$  were 4.3 and 3.3 in the geogrid section and unreinforced control sections respectively, representing a 30 % increase in the geogrid section.

Based on these results, the subgrade strength in both the geogrid and unreinforced control sections appears unusually high for Alberta conditions. Although actual embankment soil tests on this section of the highway were unavailable, pre-construction borehole results suggest a sandy material which is in line with CBR results.

#### 4. PAVEMENT DESIGN ANALYSIS AND COMPARISONS BY DIFFERENT AVAILABLE METHODS

A pavement design evaluation using AASHTOWare PavementME™ (PMED) [14] and SpectraPave™ (Spectrapave) software [15] was performed for the existing pavement that was originally designed by the AASHTO'93 [13] method. SpectraPave software was developed by Tensar and is capable of taking into account the increased layer coefficient of a granular base layer due to reinforcement. Three different design scenarios have been evaluated in this study and are discussed below:

##### 4.1 Pavement Design by AASHTO' 93

To perform the pavement design by AASHTO 93, the following inputs were used in the original design:

- Design ESALs/day/dir – 1060
- Subgrade modulus – 40 MPa, equivalent CBR – 4%
- Traffic growth factor – 3% (compounded)
- Lane distribution – 85%/15%
- 20-year Design ESALs (Outer Lane/Inner Lane) –  $8.84 \times 10^6 / 1.56 \times 10^6$
- Serviceability loss – 1.7
- Reliability – 90%
- Overall standard deviation  $S_0$  – 0.45
- Structural coefficient – 0.40 for ACP and 0.14 for crushed granular base course

Based on the above parameters, the recommended full-stage pavement structure consists of 200 mm ACP and 400 mm GBC. For staged construction, the first stage pavement structure consists of 130 mm ACP and 400 mm GBC followed by 70 mm ACP at final-stage paving.

##### 4.2 Pavement Design by SpectraPave software

A pavement design was carried out using SpectraPave and using the same design inputs as used in AASHTO'93. Additionally, the geogrid was used in the design. SpectraPave is capable of modifying the GBC layer coefficient based on the geogrid input. For full-stage pavement, the following pavement structures were produced by SpectraPave.

**Table 1: Recommended Pavement Structures for Reinforced and Unreinforced Pavement by SpectraPave™**

<b>Pavement structure</b>	<b>Geogrid Reinforced test section</b>	<b>Unreinforced control section</b>
ACP (mm)	140	200
GBC (mm)	400	400

A 60 mm ACP difference is noted between the results of the SpectraPave analysis and the AASHTO'93 design. This variance (10 percent of the total pavement thickness reduction) occurred due to a modified GBC layer coefficient of 0.197 estimated by SpectraPave. This aligns with findings from Webster [11] that the inclusion of geogrid resulted in a reduction of pavement thickness ranging from 5 percent to 40 percent depending on the pavement thickness.

SpectraPave was also used to evaluate the existing first-stage pavement. Based on the pavement thickness of 130 mm ACP and 400 mm GBC, and a modified GBC layer coefficient in the geogrid section, the calculated Structural Number (SN) for reinforced and unreinforced pavement sections are 131 mm and 108 mm respectively, and the corresponding estimated ESALs are  $7.20 \times 10^6$  and  $1.96 \times 10^6$ . These ESALs were used to back-calculate the service life. The predicted service life would be 17 years and 5.5 years for reinforced and unreinforced pavement sections respectively. However, after 5.5 years of construction, both the sections have reached a similar condition based on the performance data and final stage pavement construction is inevitable.

### 4.3 Pavement Design PMED software

The recommended pavement design thickness and all other applicable inputs from the AASHTO'93 design method were used in PMED to run the design for reinforced and unreinforced pavement sections to compare the differences in the predicted distresses. PMED Manual of Practice [14] section 3.5 states that "geogrid and other reinforcing materials cannot be simulated in PavementME design (PMED) software". However, these can be simulated by changing the resilient modulus of the unbound layers and through a calibration. The Manual of Practice does not provide guidance on how to modify the resilient modulus of the granular base when using PMED.

Studies from the literature review investigated the effects of reinforcement on aggregate bases. As reported previously, Siekmeier [8] found that the presence of a geogrid increases the resilient modulus by factors ranging from 1.0 to approximately 2.5 depending on confinement and moisture conditions. White [12] found that the presence of geogrid increased the base modulus by 22 %. Therefore, to reflect an increase in modulus, the GBC modulus for the reinforced section was increased by a factor of 1.8 which is approximately the mid-point of the increased modulus factor found in the literature review. This is higher than the 1.4 factor, based on a modified coefficient of 0.197 for GBC, from 'SpectraPave'. Tables 2 and 3 present the results of different pavement distresses for reinforced test and unreinforced control pavement sections from PMED for full-stage and first-stage pavement structures.

**Table 2: Summary of Full-Stage Pavement Structures and Distresses in Reinforced Vs. Unreinforced Section from PMED**

Hwy: Control section	AADTT	Asphalt thickness	Base thickness	GBC Mr, MPa	SG Mr, MPa	Terminal IRI (m/km)	Total Rutting (mm)	AC Rutting only (mm)	AC Bottom-up Fatigue Cracking (%)	AC Thermal Fracture (m/km)	AC top-down Fatigue Cracking (%)
63:06 (unreinforced)	1040	200	400	250	40.00	2.65	19.48	6.41	1.55	40.97	14.50
63:06 (reinforced)	1040	200	400	450	40.00	2.62	18.40	6.93	1.45	40.97	14.20
Difference in Distresses						1.13%	5.54%	-8.11%	6.45%	0.00%	2.07%

**Table 3: Summary of First-Stage Pavement Structures and Distresses in Reinforced Vs. Unreinforced Section from PMED**

Hwy: Control section	AADTT	Asphalt thickness	Base thickness	GBC Mr, MPa	SG Mr, MPa	Terminal IRI (m/km)	Total Rutting (mm)	AC Rutting only (mm)	AC Bottom-up Fatigue Cracking (%)	AC Thermal Fracture (m/km)	AC top-down Fatigue Cracking (%)
63:06 (unreinforced)	1040	130	400	250	40.00	2.71	21.46	7.16	1.61	40.97	15.64
63:06 (reinforced)	1040	130	400	450	40.00	2.66	19.69	7.44	1.45	40.97	14.94
Difference in Distresses						1.85%	8.25%	-3.91%	9.94%	0.00%	4.48%

All the predicted distresses except AC rutting are slightly higher in the unreinforced control section after 20-years of service life for both first-stage and final-stage pavement. AC rutting is a function of binder type and ACP thickness and hence is not expected to be influenced by increased GBC modulus. Considering the same construction history and material type, it is not clear why the predicted AC rutting in the geogrid reinforced section is higher (~0.5 mm) than in the unreinforced control section. Total rutting in the unreinforced control section was predicted to be more (~1.8 mm higher in the first-stage pavement), which is reasonable considering its lower base modulus. However, all the differences are insignificant and do not predict the improved performance of the geogrid reinforced section.

## 5. PERFORMANCE MONITORING AND DATA ANALYSIS

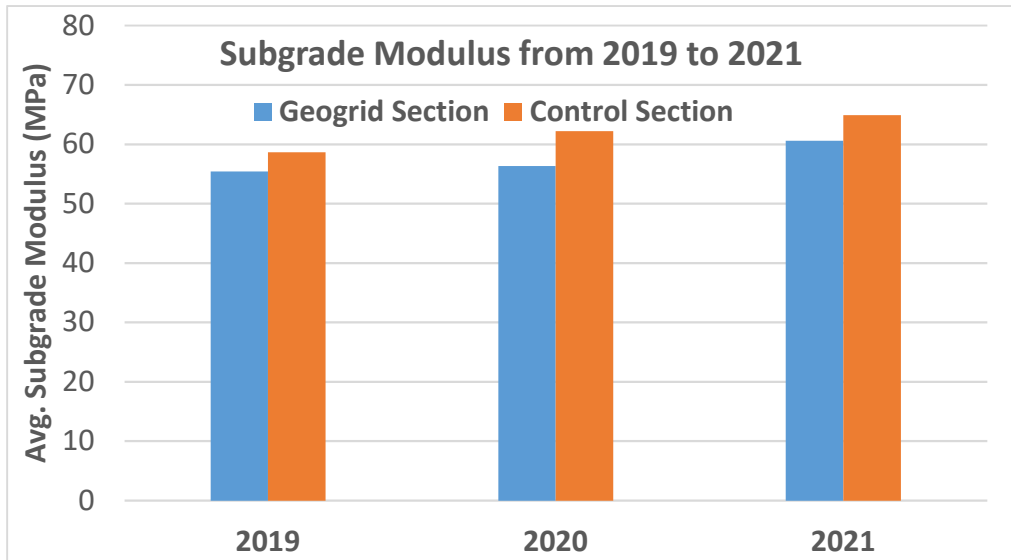
To accomplish the performance monitoring, IRI, Rut, FWD, LCMS data were collected annually since the construction in 2015. Field reconnaissance were completed every year since 2019 to document the surface condition. All collected data were analyzed. The following sections describe the outcome of the performance data analysis.

### 5.1 Falling Weight Deflectometer (FWD) Data Analysis

Due to the realignment of the chainages on Hwy 63:06 and location errors, correctly located FWD was collected starting in 2019. FWD data collected from 2019 to 2021 was analyzed using an in-house back-calculation tool.

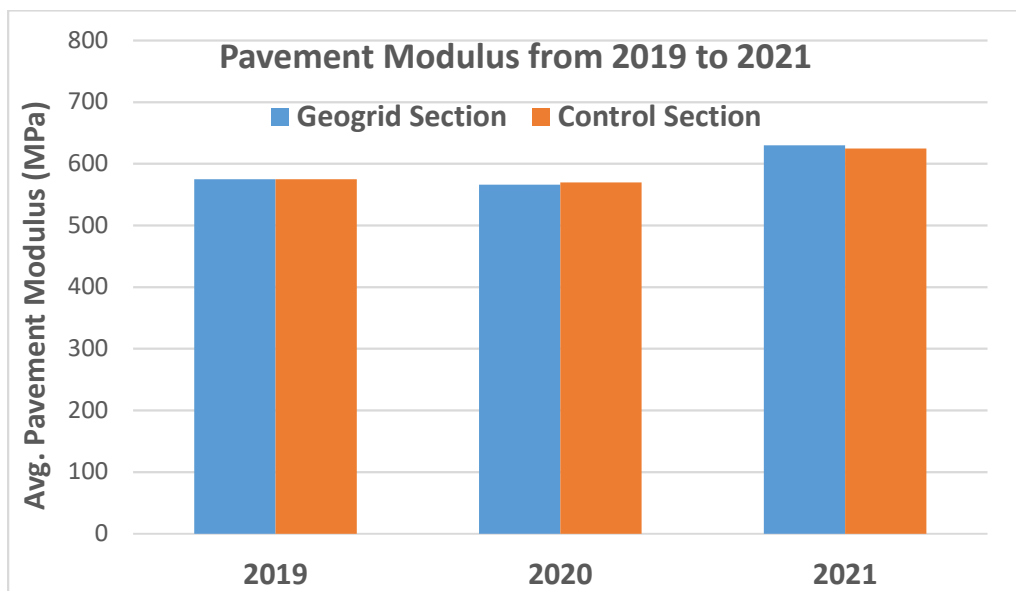


Figure 1 presents the back-calculated subgrade resilient modulus ( $M_r$ ) for geogrid and unreinforced control sections. The average existing  $M_r$  is similar in both sections and ranges between 55 MPa and 65 MPa. The  $M_r$  of the unreinforced control section is consistently higher than geogrid reinforced test section, which aligns with the APLT results.



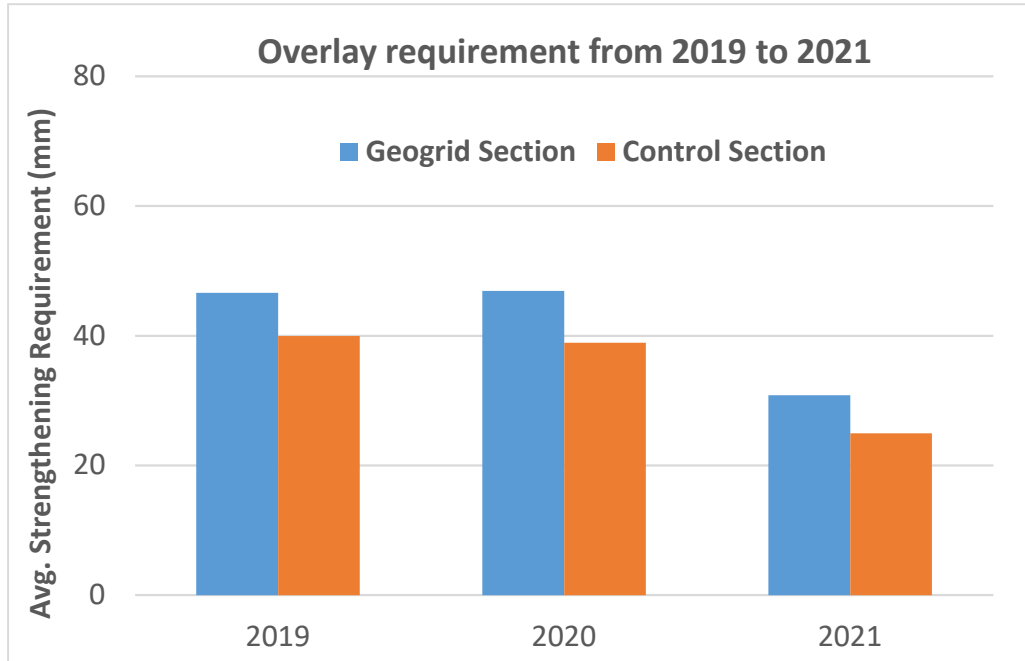
**Figure 1: Subgrade Modulus from 2019 to 2021 in Geogrid Test and Adjacent Unreinforced Control Sections**

Figure 2 presents the back-calculated pavement modulus for geogrid and adjacent unreinforced control sections. The average existing pavement modulus is alike in both sections and ranges between 550 MPa and 650 MPa.



**Figure 2: Pavement Modulus from 2019 to 2021 in Geogrid Test and Adjacent Unreinforced Control Sections**

Figure 3 shows the strengthening requirements for the geogrid and unreinforced control sections. FWD data indicates similar final paving requirements for both the geogrid reinforced test and unreinforced control sections. Changes in the strengthening requirements over time can be explained by the inherent variability of FWD as reported by McMillan et al. [16].



**Figure 3: Overlay Requirements from 2019 to 2021 in Geogrid Test and Adjacent Unreinforced Control Sections**

## 5.2 International Roughness Index (IRI) and Rut Data Analysis

IRI and Rut data collected after construction to date were analyzed. The average IRI in both sections, as presented in Figure 4, has increased consistently with time. The IRI in the geogrid reinforced test section was slightly higher than the unreinforced control section in all years except 2021. In 2021 the IRI between km 19.150 and km 19.200 in the unreinforced control section was recorded as exceptionally high and pushed up the average IRI. Localized dipped transverse cracks along with potholes contributed to the higher roughness of the entire unreinforced control section.

Average Rut in the outer wheel path (OWP), as presented in Figure 5, has generally increased with time for both unreinforced control and geogrid reinforced test sections.

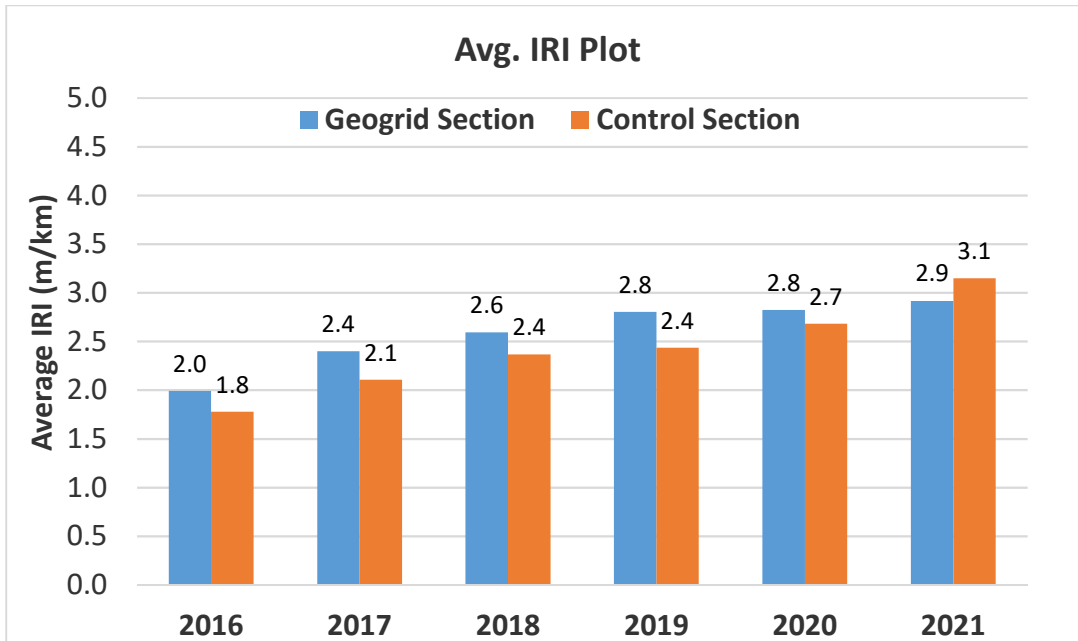


Figure 4: IRI Plots for Geogrid Test and Adjacent Unreinforced Control Section

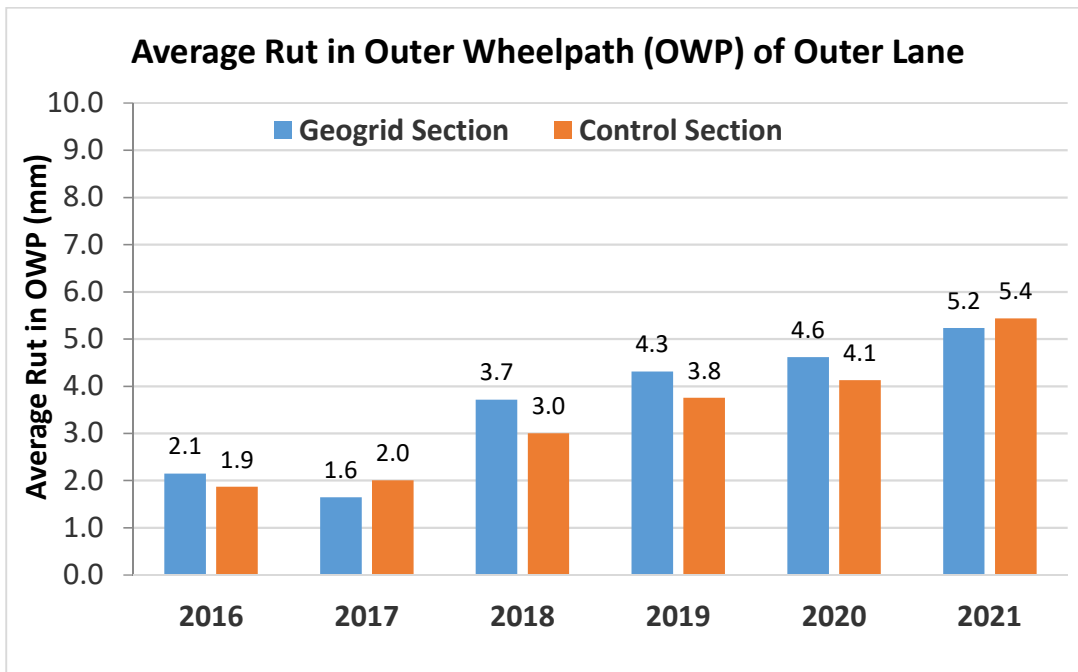


Figure 5: Average Rut Plots in the Outer Wheelpath of Outer Lane

### 5.3 Laser Crack Measurement (LCMS) Data Analysis

The LCMS data collected from 2016 to 2021 on the northbound outer driving lane was analyzed. Observations of the longitudinal and fatigue cracking, presented in figures 6 and 7 respectively, were generally consistent and increased throughout the period of data collection. The LCMS data for longitudinal and fatigue cracking were similar to what was observed from the field inspections.

The transverse cracking data from LCMS did not align with field observations and is not reported. Transverse cracking data based on visual observations is provided in section 6.

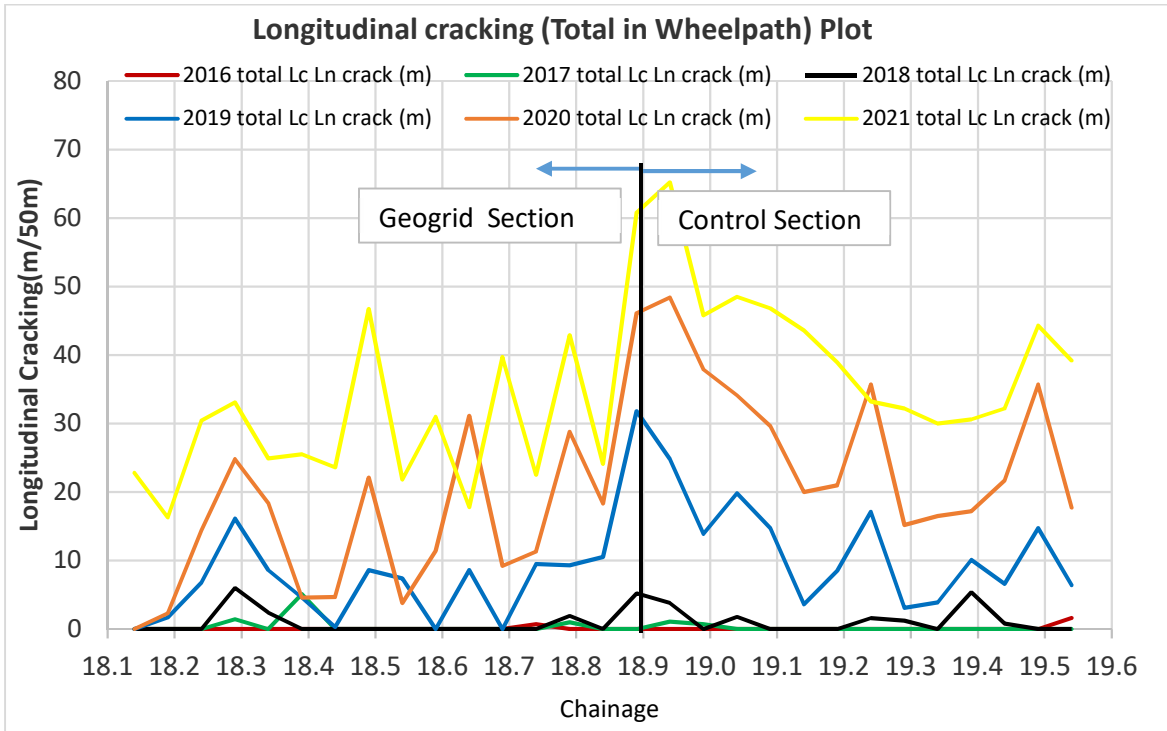


Figure 6: Longitudinal Cracking (Total in Wheelpath) Plot

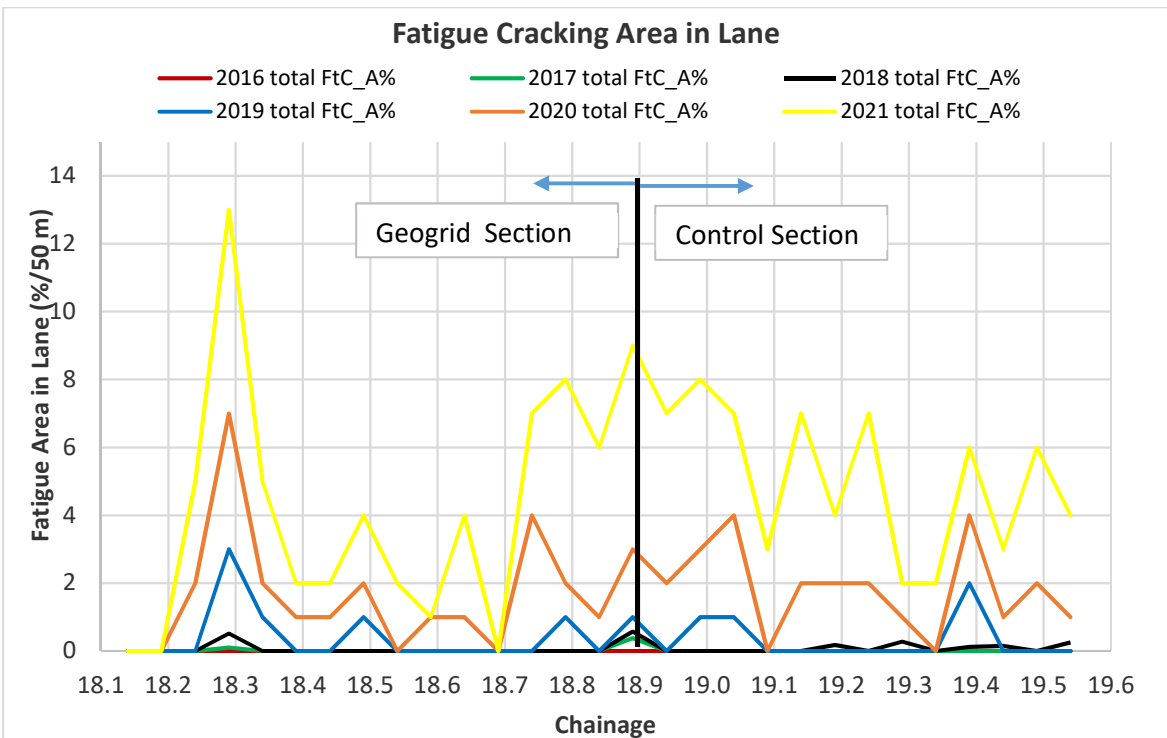


Figure 7: Fatigue Cracking Area (%) in Lane Plot

## 6. Visual Observations

After establishing the correct chainage of geogrid test and unreinforced control section, field reconnaissance was carried out for three consecutive years from 2019 to 2021 to capture the pavement surface condition. General observations for both the geogrid and unreinforced control section include the following:

- Overall pavement surface in both sections has deteriorated over time and appeared to be in the worst condition in 2021
- Similar overall pavement distresses in both sections
- General waviness in both sections
- Many segregated areas with moderate to extreme severity throughout.
- A patch was installed between km 18.500 and km 18.517 on a culvert dip in 2020. A couple of transverse cracks had reflected through the patch in 2021.

The summary of observations from the walking survey from different years is tabulated below. A few representative photos for both sections are also included.

**Table 4: Field Reconnaissance Summary**

Distress	2019		2020		2021	
	Geogrid section	Unreinforced Control section	Geogrid section	Unreinforced Control section	Geogrid section	Unreinforced Control section
Longitudinal wheel path cracking	Frequent to extensive (~63% length of the section) slight to predominantly moderate severity in OWP of the outer lane	Frequent to extensive (~61% length of the section) slight to predominantly moderate severity in OWP of the outer lane	Frequent to extensive (~63% length of the section) slight to predominantly moderate severity in OWP of the outer lane	Frequent to extensive (~61% length of the section) slight to predominantly moderate severity in OWP of the outer lane	Frequent to extensive (~100% length of the section) slight to extreme severity in OWP of the outer lane	Frequent to extensive (~100% length of the section) slight to extreme severity in OWP of the outer lane
Rutting	Negligible throughout the section except up to 10 mm localized rutting.	Negligible throughout the section.	Negligible throughout the section except up to 10 mm localized rutting.	Average rutting of 3 mm to 4 mm	Negligible throughout the section except up to 10 mm localized rutting.	Negligible throughout the section except up to 10 mm localized rutting.

Distress	2019		2020		2021	
	Geogrid section	Unreinforced Control section	Geogrid section	Unreinforced Control section	Geogrid section	Unreinforced Control section
Transverse Cracking (TC)	Six TC (full width) of slight to moderate severity. Some of the TCs were meandering	Seven TC (full width) of slight to moderate severity. Some of the TCs were moderate to extreme severity.	Ten TC (full width) of slight to moderate severity. Some of the TCs were meandering	Ten TC (full width) of mostly moderate to extreme severity and at some locations slight to moderate severity	Fifteen TC (full width) of mostly of moderate to extreme severity and at some locations slight to moderate severity	Sixteen TC (full width) of mostly moderate to extreme severity and at some locations slight to moderate severity

### Representative Photos







2019 (Geogrid Reinforced Test section)	2019 (Unreinforced Control section)
	
Photo 1: km 18.530, Meandering Transverse crack, looking south-west	Photo 2: Km 19.157, segregated area with potholes, looking west
2020 (Geogrid Reinforced Test section)	2020 (Unreinforced Control section)
TAC 	



Photo 3: Km 18.765, Segregated areas in outer wheelpath along with branched out transverse and longitudinal cracking, looking west	Photo 4: Km 19.205, Branched out TC and longitudinal cracking created fatigue cracking in outer wheel path, looking west
2021 (Geogrid Reinforced Test section)	2021 (Unreinforced Control section)
	
Photo 5: Km 18.710, General pavement condition with Branched out longitudinal cracking, looking south	Photo 6: Km 19.000, General pavement condition with Branched out longitudinal cracking, looking north

**7. CONCLUSIONS**

This study monitored the performance of a geogrid reinforced pavement test section and an adjacent unreinforced control section for six years. Condition data such as IRI, Rut, LCMS, FWD were analyzed. Field observations were also documented. The pavement design was also evaluated using SpectraPave software by Tensar and AASHTOWare Pavement ME Design (PMED). The findings from this study are summarised below.

- While plate load testing would suggest some improvement due to the geogrid reinforcement based on the base layer to subgrade Mr ratio, the results overall show an unusually strong subgrade that would not expect to benefit from the use of a geogrid.
- Based on 6 years of post-construction field observations and analysis of IRI, Rut, LCMS, and FWD data (subgrade modulus, pavement modulus, and final paving requirement) analysis, both the geogrid reinforced test and unreinforced control sections have performed similarly.
- ‘SpectraPave’ analysis predicted 10 percent (60 mm of ACP) of the total full-stage pavement thickness reduction over the service life. The first-stage pavement analysis predicted service life difference of ~12 years between reinforced and unreinforced pavement sections. However, after 6 years of construction, both the sections have reached a similar condition based on the performance data and final stage pavement construction is unavoidable.
- PMED analysis showed an insignificant performance improvement of the geogrid reinforced pavement section over six years in service.
- Potential reasons for the lack of performance difference between the reinforced and unreinforced control sections could be:
  - The strong subgrade, with CBR values that appear to be above the range of geogrid effectiveness.

- The relatively thick (400 mm) GBC layer. Deflections from the wheel loads on a thick GBC may not reach to the subgrade to activate the geogrid. However, given its freeze-thaw climate, Alberta Transportation does not design pavements with a GBC thinner than 300 mm.
- The position of the geogrid, located at the subgrade-GBC interface. This appears to be sub-optimum based on the literature review.
- The thickness of the ACP layer, at 130 mm. The literature review indicated that the ACP thickness can have a significant influence on the effects of geogrid reinforcement. However, Alberta Transportation does not generally construct thinner ACP layers (i.e. 100 to 120 mm of ACP is generally the thinnest final stage pavement thickness).

Alberta Transportation intends to continue to monitor the longer term performance of the geogrid test and unreinforced control sections, including after the final stage paving. However, based on the first 6 years and since both sections are at the end of their service life, it is not expected that there will be any performance differences over the long term.

## 8. REFERENCES

[1] Alimohammadi, H., Schaefer, V.R., Zheng, J., Li, H., 2021. "Performance evaluation of geosynthetic reinforced flexible pavement: a review of full-scale field studies". *International Journal of Pavement Research and Technology*, Vol 14, pp. 30-42

[2] Perkins, S.W., 1999, "Geosynthetic Reinforcement of Flexible Pavements: Laboratory Based Pavement Test Sections". Report No. FHWA/MT-99-001/8138. Montana Department of Transportation, Helena, MT, USA.

[3] Cancelli, A., Montanneli, F. , "In-ground test for geosynthetic reinforced flexible paved roads". .N.M.N. United States, 55101-1088. Industrial Fabrics Association International, 1996.

[4] Ibrahim, E.M., El-Badawy, S.M., Ibrahim, M.H., Gabr, A., Azam, A., 2017. "Effect of geogrid reinforcement on flexible pavements". *Innovative Infrastructure Solutions*, Article number: 54

[5] Hass, R., Walls, J., Carroll, R. G., 1988. "Geogrid Reinforcement of Granular Bases in Flexible Pavements" *Transportation Research Record 1188*, TRB, pp. 19-27

[6] Chen, Q., Abu-Farsakh, M., 2012. "Structural Contribution of Geogrid Reinforcement in Pavement" *GeoCongress 2012*© American Society of Civil Engineers 2012.

[7] Ghafoori, N., Sharbaf, M., 2016. "Use of Geogrid for Strengthening and Reducing the Roadway structural Sections", Carson City, NV, USA,

[8] Siekmeier, J., 2016. "Geogrid reinforced aggregate base stiffness for Mechanistic pavement design". Minnesota Department of Transportation Research Services & Library.

[9] Moghaddas-Nejad, F., Small, J.C., 1996. "Effect of geogrid reinforcement in model track tests on pavements". *Journal of Transportation Eng.* Vol-122, No-6, pp-468-474.



[10] Zadehmohamad, M., Luo, N., H., Abu-Farsakh, M., Voyiadjis, G., 2022. "Evaluating long-term benefits of geosynthetics in flexible pavements built over weak subgrades by finite element and Mechanistic-Empirical analyses". Volume 50 Issue 3. Elsevier, Geotextiles and Geomembranes journal.

[11] Webster, S.L., 1993. "Geogrid Reinforced Base courses for Flexible Pavements for Light Craft: Test Section Construction, Behavior under Traffic, Laboratory Tests, and Design Criteria". U.S. Army Corps of Engineers, Waterways Experiment Station. Vicksburg, MS, USA 1993.

[12] White, D., J., Vennapusa, P., Siekmeier, J., Gieselman, H., 2019. "Cyclic Plate Load Testing for Assessment of Asphalt Pavements Supported on Geogrid Stabilized Granular Foundation" GSP 310, Geo-Congress, ASCE.

[13] American Association of State Highway and Transportation Officials, AASHTO guide for design of pavement structures, AASHTO, Washington DC, USA, 1993

[14] Mechanistic-Empirical Pavement Design Guide – A manual of practice, by AASHTO, Third Edition, 2020

[15] <https://www.tensarcorp.com/solutions/design-support>

[16] McMillan, C., Lakkavalli, V., Juhasz, M., 2010. "Variation in Back Calculated Pavement Strength" Canadian Technical Asphalt Association (CTAA) Proceedings.

## Appendix 1 – Tabular Summary of Literature Review on Geosynthetics

Author	Geosynthetic tested (geogrid/Geotextile)	Type of Testing (field, lab, modelling)	Subgrade Type	Position of Reinforcement	Pavement Structures tested/modelled	Conclusions
Alimohammadi et al. [1]	This study attempted to compare the findings of a number of field studies by different investigators to evaluate the performance of geosynthetic reinforced flexible pavement					<ol style="list-style-type: none"> <li>Findings from different study indicated the main appreciable improvement of geosynthetic both geogrid and geotextile reinforcements depends on various aspects such as subgrade stiffness, base aggregate thickness and quality, ACP thickness and quality, geogrid stiffness and location.</li> <li>This study developed a formula to calculate the granular equivalent (GE) factor from FWD tests for unreinforced and geosynthetic reinforced sections of the experimental tests by various investigators</li> </ol>
Perkins S. W. [2]	Tensar BX-1100 geogrid, Tensar BX-1200 geogrid and Amoco 2006 woven geotextile	Large scale laboratory testing	<ol style="list-style-type: none"> <li>Weak subgrade - plastic clay</li> <li>Strong subgrade - silty sand</li> </ol>	<ol style="list-style-type: none"> <li>Subgrade-base interface</li> <li>100 mm up in a base layer having a thickness of 300 mm</li> </ol>	Weak subgrade - 750 mm Strong subgrade - 1000 mm GBC - 200 mm for weak subgrade GBC - 300 to 400 mm for strong subgrade ACP - 75 mm	<ol style="list-style-type: none"> <li>Structural contribution of geosynthetic reinforcement is similar to that of additional base course</li> <li>Stiffer geogrid provides better pavement performance, geogrid perform better than geotextile</li> <li>Significant better performance was observed when the geogrid was elevated in the base.</li> <li>Geosynthetic reinforcement provides important benefits when the subgrade had a CBR of 1.5 or less, and little to no benefits were noted when the subgrade had a CBR of 20 or more</li> </ol>
Cancelli at al. [3]	<ol style="list-style-type: none"> <li>Single layer biaxial geogrid</li> <li>Multiple layer biaxial geogrid</li> <li>Woven Polyester geogrid</li> <li>Slit film woven fabrics</li> <li>composite structure - extruded geogrid and non-woven geotextile</li> </ol>	Field and lab tests for subgrade CBR, Plate load test	Subgrade with varying CBR (1% to 8%)	Several reinforcement layers at different depths in GBC layer	GBC - 300 mm to 500 mm ACP - 75 mm	<ol style="list-style-type: none"> <li>Multilayer geogrids show lower deformation than the common single-layer geogrid</li> <li>Geogrid placed in the interface of subgrade and base is effective for increasing the service life of a paved road</li> <li>Structural layer coefficient of an aggregate layer can be increased by a geogrid layer having a layer coefficient ratio ranging from 1.5 to 2.0</li> </ol>
Ibrahim et al. [4]	Single layer of uniaxial geogrid	<ol style="list-style-type: none"> <li>Lab testing - Static plate loading</li> <li>Finite element analysis (FEA)</li> </ol>	Clay subgrade soils	Four different positions within GBC	Subgrade - 300 mm GBC - 150 mm ACP - 50 mm	<ol style="list-style-type: none"> <li>The optimum position of the geogrid to reduce tensile strains was found directly underneath the ACP layer and also within 33 to 50 % of the GBC layer height measured from the bottom of the GBC</li> </ol>

Author	Geosynthetic tested (geogrid/Geotextile)	Type of Testing (field, lab, modelling)	Subgrade Type	Position of Reinforcement	Pavement Structures tested/modelled	Conclusions
Hass et al. [5]	Tensar SSI geogrid	Lab testing - full-scale cyclic load and dynamic load tests	Fine grained beach sand (SP) with varying subgrade CBR (<1% to 8%)	1. Different positions in different set of tests - Bottom, mid and top of GBC layer 2. Two layers of reinforcement in weak subgrade	GBC - 100, 150, 200 and 300 mm ACP - 50 mm, 75 mm and 100 mm	1. For optimum effect, geogrid reinforcement should be placed at the base-subgrade interface of thin base sections and near the middle of thicker bases 2. The zone of geogrid placement should not involve elastic tensile strains in the geogrid that are greater than 0.2 %
Chen et al. [6]	GG1 and GG2 biaxial Geogrid GG3 and GG4 triaxial geogrid	Lab testing -cyclic load tests	Silty clay	Different positions in different tests - base/subgrade interface, mid depth of GBC and the upper one third of the base layer	Various GBC thicknesses -302 mm to 325 mm ACP -51 mm to 60 mm	1. The value of the resilient modulus of the base course layer can be increased by 10-90 percent and that the thickness of the base layer can be reduced by 12 to 49 percent for the geogrid reinforced pavement sections 2. Higher tensile modulus geogrids typically provide better performance
Ghafoori et al. [7]	Biaxial rectangular geogrid (BX1100) and Triaxial triangular (TX130S) geogrid	1. Lab testing - cyclic load tests 2. Instrumentation	Silty clay	Different positions in different tests - Subgrade/base interface and mid depth of GBC	Locally available subgrade soil - minimum 1500 mm GBC - 305 mm and 406 mm ACP -76 mm	1. The inclusion of both biaxial and triaxial geogrids in flexible pavement reduced the Asphalt surface rutting and vertical stresses at the subgrade-base interface. 2. Use of geogrid increase the number of load applications by a factor of 1.5 to 7 depending on the test section and geogrid type. 3. Using a Base Course Reduction (BCR) method and the measured rutting depth, the inclusion of geogrid resulted in the base thickness reductions of 11 to 44 percent depending on the variables.
Siekmeier et al. [8]	SS20 biaxial geogrid	Lab testing, laboratory testing combined with numerical analysis using PFC3D and MnPAVE software-	Engineered soil with different modulus	Three layers of biaxial geogrid centered within base materials in 60 mm spacing	Various thickness of engineered subgrade soil, base and asphalt layers. Engineered soil - 203 mm, 610 mm, 914 mm GBC - 203 mm, 254 mm, 305 mm Asphalt - 102 mm, 152 mm	1. Geogrid reinforcement effects varies during the year. 2. The seasonal effects to be included during implementation to allow the fatigue and rutting to be more accurately estimated over the expected pavement design life. 3. Geogrid reinforced aggregate base is likely to provide the most effective benefit when the pavement foundation materials are weak.
Moghaddas-Nejad et al. [9]	Biaxial Tensar SS2 geogrid	Model testing facility with single and multiple track test	Sand subgrade	Different positions in different set of tests - subgrade-base interface, mid depth of GBC layer	Tests were performed at approximately one-quarter scale. Subgrade - 2000 mm GBC - 40 mm ACP - 20 mm	1. Confinement and interlocking of the base materials as well as the improved load distribution on the subgrade layers are the main causes of reduction of subgrade deformation 2. For a thin base layer, the least surface deformation was obtained with the geogrid at the center of the base layer.

Author	Geosynthetic tested (geogrid/Geotextile)	Type of Testing (field, lab, modelling)	Subgrade Type	Position of Reinforcement	Pavement Structures tested/modelled	Conclusions
Zadehmohamad et al. [10]	Geogrid (single and double layer) and geotextile with three different reinforcement stiffness	Finite Element Modelling	Weak subgrade - clay soil with CBR~1.0% - 1.5%	Different positions in different set of tests - subgrade-base interface, mid depth of GBC layer	Various GBC thickness - 200 mm, 250 mm, 300 mm, and 350 mm ACP - 90 mm	<ol style="list-style-type: none"> <li>1. The inclusion of one geogrid/geotextile layer at the base-subgrade interface could significantly reduce pavement rutting.</li> <li>2. The use of geogrid is more effective than geotextile in reducing pavement rutting.</li> <li>3. Calculated Traffic Benefit Ratio (TRB) value from this study demonstrate an optimum at a base thickness of 250 mm.</li> <li>4. Superior benefits of using double geogrid layers compared to single layer cases.</li> </ol>
Webster et al. [11]	Two types of geogrid - punched sheet-drawn and woven structure	Combination of Field test sections and lab testing	Heavy clay (CH) CBR ranged 2.3% - 7.1%	Subgrade-base interface and middle of GBC	Various GBC - 50 mm to 450 mm ACP - 100 mm	<ol style="list-style-type: none"> <li>1. Geogrid performance is a function of the depth of geogrid placement</li> <li>2. The use of geogrid can reduce the total pavement design thickness</li> <li>3. The thickness reduction range from approximately 40 percent for unreinforced pavement thicknesses of 11 inches (279 mm) to 5 percent for 30 inch (762 mm) thick pavements</li> </ol>
White et al. [12]	Biaxial geogrid	Field test - cyclic plate load tests and Falling Weight Deflectometer (FWD) test	Sand to loamy sand	Geogrid at 152 mm below the bottom of AC layer	ACP - 114 mm followed by Reclaimed asphalt pavement (RAP) - 152 mm	<ol style="list-style-type: none"> <li>1. About 11 percent increase in the composite resilient modulus (<math>M_r</math>-comp) of a geogrid section than in unreinforced control section.</li> <li>2. A similar analysis of the FWD test results did not show the statistically noteworthy benefit with the inclusion of geogrid.</li> </ol>